Bloch surface wave enhanced biosensor for the direct detection of Angiopoietin-2 tumor biomarker in human plasma

Research Article | Vol. 9, No. 2 | 1 Feb 2018 | BIOMEDICAL OPTICS EXPRESS 529
Biomedical Optics EXPRESS

Bloch surface wave enhanced biosensor for the direct detection of Angiopoietin-2 tumor biomarker in human plasma

RICCARDO RIZZO,[1] MARIA ALVARO,[2] NORBERT DANZ,[3] LUCIA NAPIONE,[2,4] EMILIANO DESCROVI,[1] STEFAN SCHMIEDER,[5] ALBERTO SINIBALDI,[6] SUBINOY RANA,[7] RONA CHANDRAWATI,[7,8] PETER MUNZERT,[3] THOMAS SCHUBERT,[9] EMMANUEL MAILLART,[10] ALEKSEI ANOPCHENKO,[6,11] PAOLA RIVOLO,[1] ALESSANDRO MASCIOLETTI,[12] ERIK FÖRSTER,[3,13] FRANK SONNTAG,[5] MOLLY M. STEVENS,[7] FEDERICO BUSSOLINO,[2,14] AND FRANCESCO MICHELOTTI[6,15]

[1]*Department of Applied Science and Technology, Politecnico di Torino, C.so Duca degli Abruzzi 24, 10129 Torino, Italy*
[2]*Laboratory of Vascular Oncology, Candiolo Cancer Institute – IRCCS, Candiolo, Italy, Department of Oncology, University of Torino, Candiolo, Italy*
[3]*Fraunhofer Institute for Applied Optics and Precision Engineering IOF, Albert-Einstein-Str. 7, Jena 07745, Germany*
[4]*Present Address: Department of Applied Science and Technology, Politecnico di Torino, C.so Duca degli Abruzzi 24, 10129 Torino, Italy*
[5]*Fraunhofer Institute for Material and Beam Technology IWS Dresden, Dresden 01277, Germany*
[6]*Department of Basic and Applied Science for Engineering, Sapienza University of Rome, Via A. Scarpa 16, 00161 Rome, Italy*
[7]*Department of Materials, Imperial College London, London SW7 2AZ, UK*
[8]*Present Address: School of Chemical and Biomolecular Engineering, The University of Sydney, Sydney, NSW 2006, Australia*
[9]*KDS Raderberger GmbH, Großröhrsdorf 01900, Germany*
[10]*HORIBA Scientific, Av. de la Vauve CS 45002 - 91120 Palaiseau, France*
[11]*Present Address: Department of Physics, Baylor University, One Bear Place #97316, 76798-7316, Waco, Texas, USA*
[12]*LABOR Srl, Via G. Peroni, 00131 Rome, Italy*
[13]*Present Address: University of Applied Sciences, Department SciTec, Jena, 07745, Germany*
[14]*federico.bussolino@unito.it*
[15]*francesco.michelotti@uniroma1.it*

Abstract: Quantitative detection of angiogenic biomarkers provides a powerful tool to diagnose cancers in early stages and to follow its progression during therapy. Conventional tests require trained personnel, dedicated laboratory equipment and are generally time-consuming. Herein, we propose our developed biosensing platform as a useful tool for a rapid determination of Angiopoietin-2 biomarker directly from patient plasma within 30 minutes, without any sample preparation or dilution. Bloch surface waves supported by one dimensional photonic crystal are exploited to enhance and redirect the fluorescence arising from a sandwich immunoassay that involves Angiopoietin-2. The sensing units consist of disposable and low-cost plastic biochips coated with the photonic crystal. The biosensing platform is demonstrated to detect Angiopoietin-2 in plasma samples at the clinically relevant concentration of 6 ng/mL, with an estimated limit of detection of approximately 1 ng/mL. This is the first Bloch surface wave based assay capable of detecting relevant concentrations of an angiogenic factor in plasma samples. The results obtained by the developed biosensing platform are in close agreement with enzyme-linked immunosorbent assays, demonstrating a good accuracy, and their repeatability showed acceptable relative variations.

#309618 https://doi.org/10.1364/BOE.9.000529
Journal © 2018 Received 23 Oct 2017; revised 1 Dec 2017; accepted 7 Dec 2017; published 8 Jan 2018

Biomedical Optics EXPRESS

OCIS codes: (240.6690) Surface waves; (280.1415) Biological sensing and sensors; (280.4788) Optical sensing and sensors.

References and links

1. J. Folkman, "Angiogenesis: an organizing principle for drug discovery?" Nat. Rev. Drug Discov. **6**(4), 273–286 (2007).
2. D. Hanahan and R. A. Weinberg, "Hallmarks of Cancer: The Next Generation," Cell **144**(5), 646–674 (2011).
3. G. Bergers and L. E. Benjamin, "Tumorigenesis and the angiogenic switch," Nat. Rev. Cancer **3**(6), 401–410 (2003).
4. L. Eklund and P. Saharinen, "Angiopoietin signaling in the vasculature," Exp. Cell Res. **319**(9), 1271–1280 (2013).
5. J. H. Park, K. J. Park, Y. S. Kim, S. S. Sheen, K. S. Lee, H. N. Lee, Y. J. Oh, and S. C. Hwang, "Serum Angiopoietin-2 as a Clinical Marker for Lung Cancer," Chest **132**(1), 200–206 (2007).
6. H. Engin, Y. Üstündağ, İ. Ö. Tekin, A. Gökmen, Ş. Ertop, and S. U. İlikhan, "Plasma concentrations of angiopoietin-1, angiopoietin-2 and Tie-2 in colon cancer," Eur. Cytokine Netw. **23**(2), 68–71 (2012).
7. N. Rigamonti, E. Kadioglu, I. Keklikoglou, C. Wyser Rmili, C. C. Leow, and M. De Palma, "Role of angiopoietin-2 in adaptive tumor resistance to VEGF signaling blockade," Cell Reports **8**(3), 696–706 (2014).
8. I. Helfrich, L. Edler, A. Sucker, M. Thomas, S. Christian, D. Schadendorf, and H. G. Augustin, "Angiopoietin-2 Levels Are Associated with Disease Progression in Metastatic Malignant Melanoma," Clin. Cancer Res. **15**(4), 1384–1392 (2009).
9. A. C. Teixeira, I. R. C. Brasil, A. F. C. Torres, and F. Tavora, "The Evaluation of Angiogenesis Markers in Hepatocellular Carcinoma and Precursor Lesions in Liver Explants From a Single Institution," Appl. Immunohistochem. Mol. Morphol., (posted 23 August 2016).
10. N. Danz, A. Sinibaldi, P. Munzert, A. Anopchenko, E. Förster, S. Schmieder, R. Chandrawati, R. Rizzo, R. Heller, F. Sonntag, A. Mascioletti, S. Rana, T. Schubert, M. M. Stevens, and F. Michelotti, "Biosensing platform combining label-free and labelled analysis using Bloch surface waves," Proc. SPIE **9506**, 95060V (2015).
11. N. Yildirim, F. Long, C. Gao, M. He, H. C. Shi, and A. Z. Gu, "Aptamer-based optical biosensor for rapid and sensitive detection of 17β-estradiol in water samples," Environ. Sci. Technol. **46**(6), 3288–3294 (2012).
12. J. Verbarg, O. Hadass, P. D. Olivo, and A. Danielli, "High sensitivity detection of a protein biomarker interleukin-8 utilizing a magnetic modulation biosensing system," Sens. Actuators B Chem. **241**, 614–618 (2017).
13. Y. Zhao, X. Zhao, and Z. Gu, "Photonic Crystals in Bioassays," Adv. Funct. Mater. **20**(18), 2970–2988 (2010).
14. M. Shinn and W. M. Robertson, "Surface plasmon-like sensor based on surface electromagnetic waves in a photonic band-gap material," Sens. Actuators B Chem. **105**(2), 360–364 (2005).
15. M. Liscidini and J. E. Sipe, "Analysis of Bloch-surface-wave assisted diffraction-based biosensors," J. Opt. Soc. Am. B **26**(2), 279–289 (2009).
16. V. Paeder, V. Musi, L. Hvozdara, S. Herminjard, and H. P. Herzig, "Detection of protein aggregation with a Bloch surface wave based sensor," Sens. Actuators B Chem. **157**(1), 260–264 (2011).
17. P. Rivolo, F. Michelotti, F. Frascella, G. Digregorio, P. Mandracci, L. Dominici, F. Giorgis, and E. Descrovi, "Real time secondary antibody detection by means of silicon-based multilayers sustaining Bloch surface waves," Sens. Actuators B Chem. **161**(1), 1046–1052 (2012).
18. A. Sinibaldi, R. Rizzo, G. Figliozzi, E. Descrovi, N. Danz, P. Munzert, A. Anopchenko, and F. Michelotti, "A full ellipsometric approach to optical sensing with Bloch surface waves on photonic crystals," Opt. Express **21**(20), 23331–23344 (2013).
19. V. N. Konopsky, T. Karakouz, E. V. Alieva, C. Vicario, S. K. Sekatskii, and G. Dietler, "Photonic Crystal Biosensor Based on Optical Surface Waves," Sensors (Basel) **13**(3), 2566–2578 (2013).
20. F. Frascella, C. Petri, S. Ricciardi, L. Napione, P. Munzert, U. Jonas, J. Dostalek, F. Bussolino, C. Fabrizio Pirri, and E. Descrovi, "Hydrogel-Terminated Photonic Crystal for Label-Free Detection of Angiopoietin-1," J. Lightwave Technol. **34**(15), 3641–3645 (2016).
21. F. Frascella, S. Ricciardi, L. Pasquardini, C. Potrich, A. Angelini, A. Chiadò, C. Pederzolli, N. De Leo, P. Rivolo, C. F. Pirri, and E. Descrovi, "Enhanced fluorescence detection of miRNA-16 on a photonic crystal," Analyst (Lond.) **140**(16), 5459–5463 (2015).
22. S. Ricciardi, F. Frascella, A. Angelini, A. Lamberti, P. Munzert, L. Boarino, R. Rizzo, A. Tommasi, and E. Descrovi, "Optofluidic chip for surface wave-based fluorescence sensing," Sens. Actuators B Chem. **215**, 225–230 (2015).
23. K. Toma, E. Descrovi, M. Toma, M. Ballarini, P. Mandracci, F. Giorgis, A. Mateescu, U. Jonas, W. Knoll, and J. Dostálek, "Bloch surface wave-enhanced fluorescence biosensor," Biosens. Bioelectron. **43**, 108–114 (2013).
24. F. Frascella, S. Ricciardi, P. Rivolo, V. Moi, F. Giorgis, E. Descrovi, F. Michelotti, P. Munzert, N. Danz, L. Napione, M. Alvaro, and F. Bussolino, "A fluorescent one-dimensional photonic crystal for label-free biosensing based on bloch surface waves," Sensors (Basel) **13**(2), 2011–2022 (2013).
25. A. Sinibaldi, N. Danz, A. Anopchenko, P. Munzert, S. Schmieder, R. Chandrawati, R. Rizzo, S. Rana, F. Sonntag, A. Occhicone, L. Napione, S. De Panfilis, M. M. Stevens, and F. Michelotti, "Label-Free Detection of Tumor Angiogenesis Biomarker Angiopoietin 2 Using Bloch Surface Waves on One Dimensional Photonic

Biomedical Optics EXPRESS

Crystals," J. Lightwave Technol. **33**(16), 3385–3393 (2015).
26. A. Sinibaldi, C. Sampaoli, N. Danz, P. Munzert, L. Sibilio, F. Sonntag, A. Occhicone, E. Falvo, E. Tremante, P. Giacomini, and F. Michelotti, "Detection of soluble ERBB2 in breast cancer cell lysates using a combined label-free/fluorescence platform based on Bloch surface waves," Biosens. Bioelectron. **92**, 125–130 (2017).
27. R. Rizzo, M. Alvaro, N. Danz, L. Napione, E. Descrovi, S. Schmieder, A. Sinibaldi, R. Chandrawati, S. Rana, P. Munzert, T. Schubert, E. Maillart, A. Anopchenko, P. Rivolo, A. Mascioletti, F. Sonntag, M. M. Stevens, F. Bussolino, and F. Michelotti, "Bloch surface wave label-free and fluorescence platform for the detection of VEGF biomarker in biological matrices," Sens. Actuators B Chem. **255**, 2143–2150 (2018).
28. D. J. Ehresman, J. W. Froehlich, G. W. Olsen, S.-C. Chang, and J. L. Butenhoff, "Comparison of human whole blood, plasma, and serum matrices for the determination of perfluorooctanesulfonate (PFOS), perfluorooctanoate (PFOA), and other fluorochemicals," Environ. Res. **103**(2), 176–184 (2007).
29. J. Treviño, A. Calle, J. M. Rodríguez-Frade, M. Mellado, and L. M. Lechuga, "Determination of human growth hormone in human serum samples by surface plasmon resonance immunoassay," Talanta **78**(3), 1011–1016 (2009).
30. M. Verstraete, A. Debucquoy, J. Dekervel, J. van Pelt, C. Verslype, E. Devos, G. Chiritescu, K. Dumon, A. D'Hoore, O. Gevaert, X. Sagaert, E. Van Cutsem, and K. Haustermans, "Combining bevacizumab and chemoradiation in rectal cancer. Translational results of the AXEBeam trial," Br. J. Cancer **112**(8), 1314–1325 (2015).
31. P. Yeh, A. Yariv, and C.-S. Hong, "Electromagnetic propagation in periodic stratified media I General theory*," J. Opt. Soc. Am. **67**(4), 423–438 (1977).
32. E. Yablonovich, "Inhibited Spontaneous Emission in Solid-State Physics and Electronics," Phys. Rev. Lett. **57**, 8–11 (1986).
33. S. John, "Strong localization of photons in certain disordered dielectric superlattices," Phys. Rev. Lett. **58**(23), 2486–2489 (1987).
34. C. Wächter, R. Rizzo, F. Michelotti, P. Munzert, and N. Danz, "Leaky waveguides for low k-measurement: From structure design to loss evaluation," Proc. SPIE **9750**, 975019 (2016).
35. P. Munzert, N. Danz, A. Sinibaldi, and F. Michelotti, "Multilayer coatings for Bloch surface wave optical biosensors," Surf. Coat. Tech. **314**, 79–84 (2017).
36. A. Anopchenko, A. Occhicone, R. Rizzo, A. Sinibaldi, G. Figliozzi, N. Danz, P. Munzert, and F. Michelotti, "Effect of thickness disorder on the performance of photonic crystal surface wave sensors," Opt. Express **24**(7), 7728–7742 (2016).
37. J. Homola, "Surface plasmon resonance sensors for detection of chemical and biological species," Chem. Rev. **108**(2), 462–493 (2008).
38. R. Rizzo, N. Danz, F. Michelotti, E. Maillart, A. Anopchenko, and C. Wächter, "Optimization of angularly resolved Bloch surface wave biosensors," Opt. Express **22**(19), 23202–23214 (2014).
39. A. Sinibaldi, N. Danz, E. Descrovi, P. Munzert, U. Schulz, F. Sonntag, L. Dominici, and F. Michelotti, "Direct comparison of the performance of Bloch surface wave and surface plasmon polariton sensors," Sens. Actuators B Chem. **174**, 292–298 (2012).
40. T. Scientific, "Dylight 650," https://www.thermofisher.com/it/en/home/life-science/protein-biology/protein-labeling-crosslinking/protein-labeling/fluorescent-protein-labeling/dylight-fluors-technology-product-guide.html.
41. N. Danz, R. Waldhäusl, A. Bräuer, and R. Kowarschik, "Dipole lifetime in stratified media," J. Opt. Soc. Am. B **19**(3), 412–419 (2002).
42. A. Sinibaldi, A. Fieramosca, R. Rizzo, A. Anopchenko, N. Danz, P. Munzert, C. Magistris, C. Barolo, and F. Michelotti, "Combining label-free and fluorescence operation of Bloch surface wave optical sensors," Opt. Lett. **39**(10), 2947–2950 (2014).
43. S. Fiorilli, P. Rivolo, E. Descrovi, C. Ricciardi, L. Pasquardini, L. Lunelli, L. Vanzetti, C. Pederzolli, B. Onida, and E. Garrone, "Vapor-phase self-assembled monolayers of aminosilane on plasma-activated silicon substrates," J. Colloid Interface Sci. **321**(1), 235–241 (2008).
44. M. Ballarini, F. Frascella, F. Michelotti, G. Digregorio, P. Rivolo, V. Paeder, V. Musi, F. Giorgis, and E. Descrovi, "Bloch surface waves-controlled emission of organic dyes grafted on a one-dimensional photonic crystal," Appl. Phys. Lett. **99**(4), 043302 (2011).
45. I. Krämer and H.-P. Lipp, "Bevacizumab, a humanized anti-angiogenic monoclonal antibody for the treatment of colorectal cancer," J. Clin. Pharm. Ther. **32**(1), 1–14 (2007).
46. G. J. Caine, A. D. Blann, P. S. Stonelake, P. Ryan, and G. Y. H. Lip, "Plasma angiopoietin-1, angiopoietin-2 and Tie-2 in breast and prostate cancer: a comparison with VEGF and Flt-1," Eur. J. Clin. Invest. **33**(10), 883–890 (2003).
47. H. Engin, Y. Ustündağ, I. Ozel Tekin, and A. Gökmen, "Plasma concentrations of Ang-1, Ang-2 and Tie-2 in gastric cancer," Eur. Cytokine Netw. **23**(1), 21–24 (2012).
48. D. J. O'Shannessy and D. J. Winzor, "Interpretation of deviations from pseudo-first-order kinetic behavior in the characterization of ligand binding by biosensor technology," Anal. Biochem. **236**(2), 275–283 (1996).
49. Y. Wang, A. Brunsen, U. Jonas, J. Dostálek, and W. Knoll, "Prostate specific antigen biosensor based on long range surface plasmon-enhanced fluorescence spectroscopy and dextran hydrogel binding matrix," Anal. Chem. **81**(23), 9625–9632 (2009).
50. H. Vaisocherová, K. Mrkvová, M. Piliarik, P. Jinoch, M. Steinbachová, and J. Homola, "Surface plasmon

Biomedical Optics EXPRESS

resonance biosensor for direct detection of antibody against Epstein-Barr virus," Biosens. Bioelectron. **22**(6), 1020–1026 (2007).

1. Introduction

Tumor angiogenesis has been one of the most intensively studied areas of cancer research in recent years. Angiogenesis – the formation of new blood vessels from pre-existing ones – has an essential role in development, as well as in tissue repair and remodeling. In adults, angiogenesis can also occur in a number of pathological conditions including neoplastic disease [1]. Indeed, after reaching a diffusion-limited size, many tumors rely on an angiogenic switch, rendering tumor angiogenesis one of the hallmarks of cancer [2,3]. Released angiogenic factors establish a dynamic tumor microenvironment where intricate intracellular paths lead to the phenotypic changes required to sustain tumor growth.

The angiogenic factor Angiopoietin-2 (Ang2) has been widely investigated due to its function in tumor vasculature and in other pathological conditions associated with endothelial dysfunction [4]. Particularly, in angiogenic tissues such as tumors, endothelial cells secrete high levels of Ang2 that promotes angiogenesis in addition to other proangiogenic factors such as vascular endothelial growth factor (VEGF). Ang2 levels are elevated in the plasma of cancer patients compared to healthy subjects; furthermore higher circulating Ang2 levels may correlate with a more advanced stage of the disease and/or a worse prognosis in some cancer types [5–8]. Ang2 may also assist in the diagnosis of difficult lesions [9]. Monitoring Ang2, as well as other angiogenic factors, is therefore desirable for disease diagnosis and future development of targeted anti-angiogenesis therapy in cancer and other diseases.

Performing an effective shift from qualitative to quantitative biology requires new innovative techniques, new approaches and close interdisciplinary collaboration among biologists, physicists, engineers, mathematicians, chemists, and computer scientists. Building on this concept, we developed an optical biosensing system that is able to detect Ang2 using a tandem approach exploiting both label-free and fluorescence detection [10]. Such a system is composed of a fast and reliable analytical instrument with integrated microfluidics and of low-cost disposable one dimensional photonic crystal (1DPC) biochips. Previous work demonstrated the detection of high concentration of Ang2 in buffer [10]. Alternative fluorescence based sensor approaches recently reached detection below 1 ng/ml concentration [11] that have been further decreased by combining fluorescence and magnetic labelling [12]. The present work targets the ng/ml concentration range while offering to analyze different biomarkers and references simultaneously in microliter sample volumes and in less time compared to ELISA assays. ELISA is considered as reference for our assay to demonstrate the clinical application of the biosensing platform requires by detecting biomarker at biologically relevant concentrations in clinical samples.

In general, the advent of biosensors based on photonic crystals and their improvements allowed the realization of simple and low-cost bioassays [13]. Indeed, during the last decade Bloch surface waves (BSW) sustained by 1DPC have been considered as a viable alternative to surface plasmon polaritons in both label-free [14–20] and fluorescence [21–23] optical biosensors. The most interesting feature of BSW relies on the enhanced and confined electromagnetic field in close proximity of the interface, leading to an increase of the label-free resolution and of the fluorescence excitation rate of fluorophores located at the 1DPC surface.

Here, we present the detection of both Ang2 spiked in buffer and endogenous Ang2 biomarker directly from human blood plasma, with the sensing platform operating in the fluorescence mode only. While several BSW based biosensors [19,22,24–27] were reported for the detection of different analytes, their accuracy was never tested with real clinical samples. Blood plasma, together with serum, is one of the main sources of clinical analytes [28]. Although it may contain many disease biomarkers, it is one of the most complex analytical matrices, in which the analytes are mixed with a large number of other molecules

Biomedical Optics EXPRESS

[29]. This represents a serious obstacle for the development of clinical biosensors handling human plasma samples.

To the best of our knowledge this is the first BSW biosensor assay for the detection of an angiogenic factor (Ang2) whose accuracy has been assessed with patients' plasma samples at clinically relevant concentrations. The results reported here, which are still limited to a small number of samples and are being extended in our present studies, can lead to a biosensing system, which allows the detection of Ang2 biomarker comparable with analytical quality laboratory methods such as enzyme-linked immunosorbent assay (ELISA). In addition, our method excludes any sample pretreatment, features short experimental time and is relatively simple to use [30].

2. BSW biochips

1DPC are photonic bandgap dielectric structures [31] characterized by a spatial periodicity of the real dielectric constant along one direction. Depending on the dielectric contrast and geometry, such structures can localize the electromagnetic field in a confined region and enhance linear and nonlinear optical effects [32,33]. The biochips used in the present work were fabricated by depositing purposely designed 1DPC directly on molded plastic substrates. In Fig. 1(a), we show a photograph of a biochip [27] together with its microfluidic cover. The substrate includes an integrated coupling prism operating in the Kretschmann-Raether configuration under total internal reflection (TIR) conditions. Such approach leads to a disposable and low-cost sensor unit, which is advantageous to the practical applications.

The substrates were fabricated by injection moulding and made out of the thermoplastic COC polymer (Topas 6013, Topas Advanced Polymers), with refractive index is $n_{SUB} = 1.530$ at $\lambda = 670$ nm. This is a clear amorphous non-polar polymer with low water adsorption, good chemical resistance, high purity and a non-reactive surface. The last point is essential for the desired biomedical application. As shown in Fig. 1(a), the substrate is equipped with a two-components injection moulded flow cell. During the fabrication, in a first step, the hard cover is moulded and, in a second step, injection of an elastomer creates a contact layer, with one micro channel that runs along the sensing surface, and forms o-rings at the top of the cell. Such elastomer ensures proper sealing of the fluidic contacts when the complete biochip is inserted in the read-out system. The fluidic channel is 800 µm wide, 100 µm high, and 27 mm long, and contains approximately 2.2 µl volume.

The 1DPCs were fabricated by depositing alternating low and high refractive index layers with optimized thicknesses. Either SiO_2 (silica) or Ta_2O_5 (tantala) and TiO_2 (titania) were used as low and high index materials, respectively. The complex refractive indices of these materials were determined by ellipsometry, making use of test multilayers sustaining BSW [34] at the wavelength $\lambda = 670$ nm: $n_{SiO2} = 1.474 + i5E\text{-}6$, $n_{Ta2O5} = 2.160 + i5E\text{-}5$, $n_{TiO2} = 2.28 + i1.8E\text{-}3$.

The design of the 1DPC used in the present work is presented in Fig. 1(b). The first silica layer of 275 nm was deposited to promote the adhesion of the stacks to the plastic substrate. The 1DPC has a periodic part made of two tantala/silica ($d_{Ta2O5} = 120$ nm, $d_{SiO2} = 275$ nm) bilayers with the top thin bilayer made of titania/silica ($d_{TiO2} = d_{SiO2} = 20$ nm).

The direct deposition of the 1DPC on the plastic substrates was carried out by means of an APS904 coating system (Leybold Optics) under high vacuum conditions [35]. The technique allows the deposition of dense coatings without substrate heating. The film densification was performed by the APS plasma ion source, which emits high energetic Ar-ions during the evaporation process in order to densify the growing film. By varying the ion energy the film densification can easily be adjusted, for example to balance intrinsic film stress. Ion energies of approximately 100 eV were applied for SiO_2 with a deposition rate 0.5 nm/s and for Ta_2O_5 with 0.4 nm/s. For the thin TiO_2 layer 120 eV and 0.25 nm/s were used. The deposition chamber was adapted to coat 90 substrates in one run with high thickness uniformity [36].

Biomedical Optics EXPRESS

The BSW biochips were designed to operate in two detection modes. In the label-free mode, similar to surface plasmon resonance (SPR) [37], the resonant dip appearing in the TIR angular spectrum as a signature of the excitation of a BSW is tracked as a function of time to measure the change of the refractive index at the biochip's surface due to binding of Ang2 biomarkers. In the fluorescence based approach, the BSW field enhancement at the biochip surface is used to amplify the fluorescence of the labelled antibodies in a sandwich Ang2 immunoassay [38]. In Fig. 1(b)-1(d), we summarize the results of numerical simulations carried out for the proposed BSW biochips, to identify the advantages arising from their use in both the detection modes. Figure 1(c) shows the theoretical reflectance in the Kretschmann-Raether TIR configuration in water environment, for both TE and TM polarizations. The simulations were performed using the transfer matrix method, for the two illumination wavelengths used in the label-free (λ_1 = 670 nm, red curves) and fluorescence (λ_2 = 635 nm, blue curves) mode. In the TE case (solid), a sharp resonant dip is observed, corresponding to the excitation of a BSW. Figure 1(b) depicts the transverse $|E|^2$ field distribution (solid) at resonance for the TE polarized BSW, compared to the bare substrate/water interface case (dashed, plotted only in the external medium). The strong field intensity enhancement and the evanescent tail in the external medium make BSW extremely sensitive to the perturbations of the refractive index at the 1DPC/water interface. In previous works, we demonstrated that the reduced linewidth ($\Delta\theta$~0.06 deg) allows a better label-free resolution compared to the SPR ($\Delta\theta$ ~1.5 deg) [39]. Figure 1(c) shows the presence of a TM polarized BSW (dashed line) with much shallower resonance owing to a weaker field localization at the 1DPC surface, where most of the 1DPC losses occurs (TiO_2 layer).

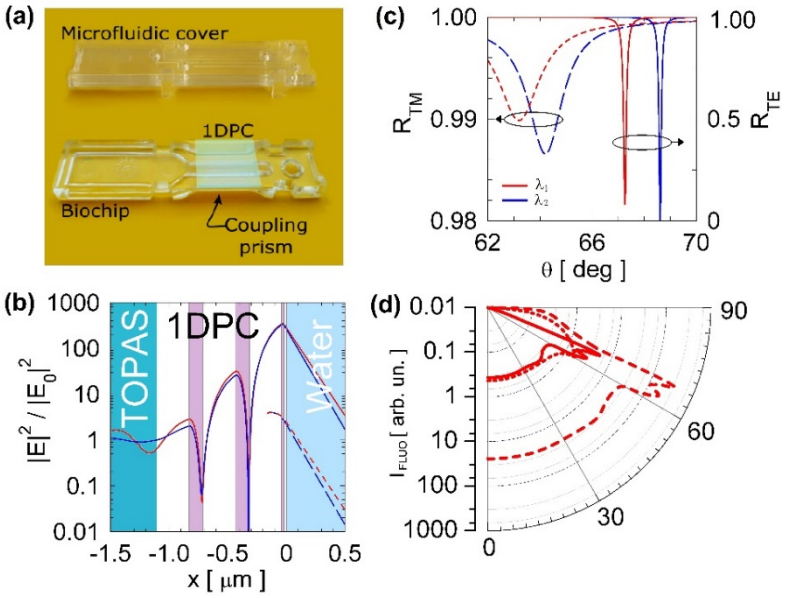

Fig. 1. (a) Picture of the plastic biochip with integrated micro-optics and polymeric microfluidic cover, the deposited PC appears as a greenish square. (b) Normalized $|E|^2$ field distribution in log scale associated to a resonantly excited TE BSW (solid) compared to the substrate/water interface (dashed). The curves are calculated at λ_1 = 670 nm (red) and λ_2 = 635 nm (blue). The 1DPC structure is shown in the background of the figure. (c) Angular reflectance spectra for the TE (solid) and TM (dashed) polarization, calculated at λ_1 (red) and λ_2 (blue). (d) Angular emission patterns in log scale integrated over the DyLight 650 spectrum and over the two TE and TM polarizations. The curves are for molecules isotropically oriented and located at the interface between: (dot) substrate/external medium, (solid) 1DPC/external medium, (dashed) 1DPC/external medium and taking into account the effect of the intensity enhancement on the excitation rate.

Biomedical Optics EXPRESS

Fluorescence operation takes advantage of the electric field enhancement to excite labelled biomolecules bound at the 1DPC surface by a second TE polarized laser beam at λ_2 = 635 nm and to force their emission into the substrate in a narrow angular range. With reference to Fig. 1(b)-1(c), due to the BSW dispersion, the resonant dip at λ_2 is shifted to larger θ, whereas the field distribution is much similar to that calculated at λ_1. In Fig. 1(d) we show the angular emission pattern I_{FL} in the substrate, for DyLight 650 dye molecules [40] placed at the 1DPC/water interface. The patterns were calculated by using dyadic Green's functions to describe the effects classically [41], assuming isotropically oriented dye molecules and integrating over the whole emission spectrum of the dye. The pattern (solid line) is compared to that obtained for dyes placed at a single substrate/water interface (dotted line), putting into evidence the enhanced emission into a narrow angular range. The pattern can be re-scaled (dashed line) by taking into account the TE excitation intensity enhancement, due to the BSW resonant excitation at λ_2. The enhancement factor (~65) was calculated as the ratio of the TE field intensities at the 1DPC/water and substrate/water interfaces, respectively at the BSW resonance and at the TIR edge. It can be observed that the combination of fluorescence excitation enhancement and angular redistribution results in a strong increase of fluorescence in a restricted angular range (62-70 deg), characterized by two bands due to either TE or TM components [42].

3. Surface chemistry, antibody immobilization and assay parameters

3.1 Reagents

Sulfuric acid (95-98%), hydrogen peroxide (30% in H_2O), (3-aminopropyl)triethoxysilane (APTES, 99%), ethanol (99.8%), glutaraldehyde solution (grade I, 50% in H_2O), sodium bicarbonate (99.7%), sodium cyanoborohydride (95%), hydrogen chloride (2 M), glycine (98.5%), bovine serum albumin (BSA, 98%), fetal bovine serum (FBS) and Dulbecco's Phosphate Buffered Saline 1X (D-PBS) were purchased from Sigma-Aldrich and used as received. Dulbecco's modified Eagle medium (DMEM) was purchased from Lonza. NeutrAvidin Protein DyLight 650 (1 mg/mL) (NeutrAvidin 650) was purchased from Thermo Fisher Scientific. Anti-human Angiopoietin-2 (Anti-Ang2) capture antibody, biotinylated anti-human Angiopoietin-2 detection antibody (Anti-Ang2*), anti-human VEGF capture antibody (Anti-VEGF), recombinant human Angiopoietin-2 protein (97%), and human Angiopoietin-2 Quantikine ELISA Kit were purchased from R&D System. Water was purified by a Millipore device.

3.2 Immobilization procedures

The immobilization procedure started with surface chemical functionalization of the 1DPC biochips carried out by APTES chemistry and taking advantage of the last 20 nm thick SiO_2 layer [43]. Before APTES, the biochips' surface was cleaned with piranha (H_2SO_4:H_2O_2 = 3:1) for 10 minutes, washed thoroughly using de-ionized (DI) water and ethanol and dried with N_2. The clean biochips were dipped in a 2% (v/v) solution of APTES in a mixture of ethanol/water (95:5 v/v) for 1 hour and then dipped in pure ethanol and sonicated three times. After rinsing with pure ethanol and drying with N_2 we baked the biochips on a hot plate at 110 °C for 1 hour. The efficiency of the functionalization was checked by contact angle measurements and immunodetection assays.

Glutaraldehyde (GAH) was used as a homobifunctional agent to couple the APTES-functionalized surface with the antibodies to be immobilized on the surface. The prepared biochips were dipped in a solution of 1% (v/v) GAH in 100 mM sodium bicarbonate buffer (pH 8.5) in the presence of 0.1 mM $NaCNBH_3$ for 1 hour. A last sonication was performed in DI water followed by a thorough wash with DI water.

Incubation of specific and non-specific monoclonal antibodies was carried out by means of a five-channel Polydimethylsiloxane (PDMS) flow cell used for wet spotting. The channels

Biomedical Optics EXPRESS

are 200 µm wide, 200 µm high and are separated by a 200 µm PDMS wall. They can be filled and emptied with protein solutions to be immobilized by using a standard microliter pipette.

This strategy allows to define signal (positive) and reference (negative) spots on the biochip surface along the illumination strip, as shown in Fig. 2. The on-chip references are used to subtract any signal that arises from non-specific binding events.

Two channels were used to incubate 20 µg/mL of the anti-Ang2 capture antibody (signal spots, positive), two channels were filled with 20 µg/mL of the anti-VEGF antibody (reference spots, negative) and one was dedicated to BSA, 10 mg/mL, (reference spot, negative). The volume used was 20 µL for each channel. The immobilization step lasted 1 hour. After the removal of the spotting tool, the biochips were rinsed with D-PBS and incubated overnight in a solution of 10 mg/mL of BSA in D-PBS at 4 °C, in order to block the surface. Four biochips were prepared at a time. All concentrations, volumes and times of the functionalization and immobilization procedures were adjusted to obtain the best sensor performance.

After the immobilization procedure, each 1DPC biochip was topped with the microfluidic cover shown in Fig. 1(a) and mounted on the platform. Before starting any assay, 1 mL of glycine-HCl (20 mM, pH 2.5) was injected and recirculated for 10 minutes to remove from the surface any not-covalently bound BSA biomolecule, which could overlay the capture antibodies.

4. Read-out system

The optical layout of the platform was designed to operate either detecting the angular reflectance at λ_1 or exploiting the BSW field enhancement when exciting at λ_2 and detecting BSW coupled fluorescence, peaked around λ_1, from DyLight 650 labelled antibodies in a sandwich Ang2 immunoassay [10]. However, the estimated limit of detection (LoD) of the label-free operation (about 11 ng/mL) is not sufficient for the detection of Ang2 at very low and clinically relevant concentrations, whereas the estimated LoD of the fluorescence mode (about 1 ng/mL) falls within the relevant range [27]. Therefore, in the present work we carried out Ang2 detection assays in the fluorescence mode only. Nevertheless, the label-free operation provides useful information on kinetic constants and affinity, for assays carried out at larger concentrations. It should be noted that the LoD strongly depends on surface chemistry and capture/detection antibody affinity. Therefore, depending on the types of cancer biomarkers and immunoassays, the same label-free scheme can provide a lower, and clinically relevant, LoD [26].

Given that we focus on the fluorescence mode, here the optical layout for label-free mode is only briefly described. Label-free operation is achieved through a TE polarized laser beam at λ_1 that is focused by a cylindrical lens into the polymer chip, thus illuminating a line at the sensor surface. The reflected light is angularly imaged onto the CCD image sensor and the BSW resonant dip is tracked as a function of time.

In Fig. 2, we sketch the optical system used in the fluorescence mode of operation. The collimated beam of a laser diode at λ_2 is focused by means of the cylindrical excitation lens (EL) into the chip, thus generating an excited line (sensing area indicated in blue in Fig. 2). The excitation beam can be laterally scanned to change the illumination angle and to ensure matching to the BSW resonance angle at λ_2 (compare Fig. 1(c)). Such a scanning of the illumination angle allows for compensating refractive index induced shifts of the resonance position during an assay. A filter set including excitation and emission filters (not shown) and a dichroic splitter (SP) are used to adjust the correct position of the illumination line and to separate excitation and emission spectral ranges.

The detection of fluorescence generated on top of the chip surface is achieved by two cylindrical optical systems. First, a system of cylindrical lenses (indicated by L1 and L2 in Fig. 2) images a 5 mm long part of the illuminated line onto the short axis of a CCD sensor. This approach reaches a lateral resolution below 100 µm to allow for simultaneously

Biomedical Optics EXPRESS

analyzing up to 20 spots. In the present work, five different measurement regions have been used only. Second, the angular spectrum of emission is imaged by means of a cylindrical Fourier lens (FL) onto the long axis of the CCD sensor. As fluorescence is coupled to BSW, each wavelength component of the spectrum is emitted at a different angle due to the dispersion of the BSW [10,42,44]. The observed angular range in the fluorescence mode is increased to approximately 8 deg, compared to 2.9 deg in the label-free mode, by introducing a cylindrical angular zoom lens (AZ). Therefore, almost all the fluorescence energy emitted into the BSW dispersion by the DyLight 650 labels is detected.

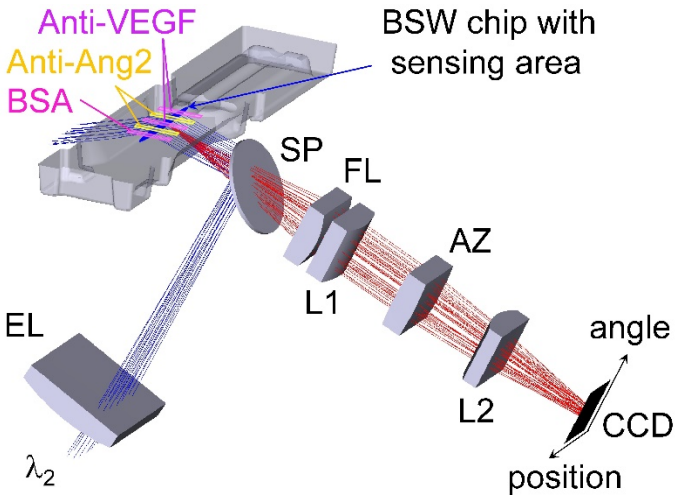

Fig. 2. Sketch of the fluorescence mode optical system without plotting laser diode collimation. Fluorescence excitation (blue) and emission (red) are shown with an arrangement of five spots along the illuminated line. The positive (Anti-Ang2) and negative regions (Anti-VEGF and BSA) were obtained with the five-channel functionalization flow cell on top of the biochip. The two axes of the CCD detector represent the position along the illuminated line on the chip as well as the angular spectrum of emission.

The CCD sensor mounted in the detection system is an APOGEE Ascent with Sony ICX814, with a 3388x2712 pixel matrix. The lasers are from Hitachi: HL6714 (λ_1) and HL63133DG (λ_2). The filter set is from Chroma: excitation filter ZET 635/20, bandpass emission filter ET 685/70; dichroic beam 45 deg splitter (SP) ZT 640 rdc. Lenses are ar-coated in the visible range. Lateral scanning of the fluorescence excitation laser is provided by a motorized stage from Thorlabs.

In case dyes emitting in a different spectral range are used ((e.g., Atto532, AlexaFluor532)), the operation principle of the platform does not change. One could adapt the 1DPC design and the operation wavelength of the label-free operation mode.

5. Results

5.1 Biological samples

Plasma samples were collected at the Candiolo Cancer Institute – IRCCS (Italy), in accordance with the protocol approved by the Institute's Ethical Commission and the Ethical Committee Piedmont Region, Torino (Italy). As inclusion criteria, the protocol considered patients with metastatic colon cancer, in treatment with bevacizumab [45] in combination with other chemotherapy agents, and having signed the informed consent. Blood sampling was done before, during, and after the therapy.

Plasma was prepared by centrifugation of the whole blood contained in the test tube with EDTA as anticoagulant; after centrifugation the corpuscular fraction was discarded and the supernatant was collected, aliquoted and stored at –80°C.

Biomedical Optics EXPRESS

5.2 Immunoassay format

When a sample solution flows over a bio-conjugated biochip (Fig. 3(a)), Ang2 target molecules can be captured at the surface (Fig. 3(b)) and results in a shift of the BSW resonance that can be detected in the label-free mode. For fluorescence operation, we injected in the biochip a biotinylated anti-Ang2* detection antibody solution, followed by fluorescence background measurement and labelling of the antibody by injecting an appropriate fluorophore (NeutrAvidin Protein DyLight 650, Fig. 3(c)). The biochip is finally washed by flowing D-PBS and fluorescence detection is performed in D-PBS upon excitation at λ_2 (Fig. 3(d)). The overall duration of the assay is 30 minutes.

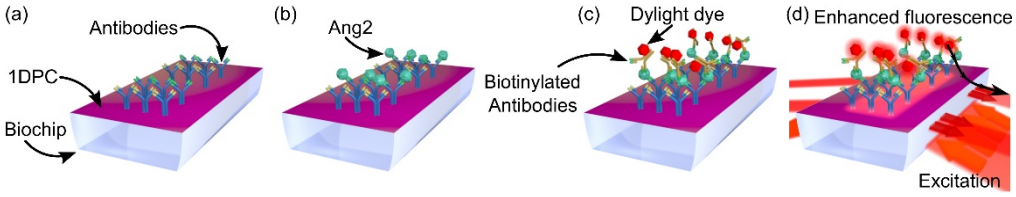

Fig. 3. Schematic of the sandwich assay for the detection of Ang2 biomarker using the fluorescence mode.

In all assays the concentration of both anti-Ang2* and NeutrAvidin 650 solutions was 1 µg/mL in D-PBS. The volume of all solutions used, from that containing the target biomarker to that used for dye labelling, was 400 µL. All solutions were recirculated for 10 minutes by forth and back pumping. The flow rate for all the injection and recirculation steps was 30 µL/min. Between each assay step, the microfluidic channel was rinsed with abundant D-PBS increasing the flow rate to 50 µL/min.

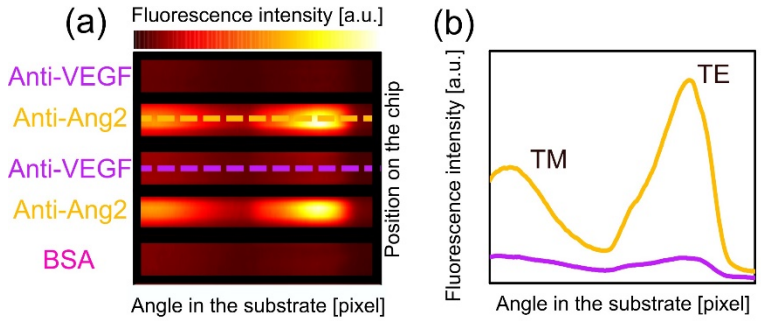

Fig. 4. (a) Fluorescence emission recorded by the CCD camera at the end of an assay, where Ang2 was detected; (b) Angular emission profiles along the dashed lines.

Figure 4(a) displays the image provided by the CCD sensor at the end of an assay, in which a solution containing Ang2 was injected in the biochip. Fluorescence intensity is collected over the 8 deg angular range. A clear fluorescence signal emerges from spots that are bio-conjugated with anti-Ang2, while signal collected from the reference spots is negligible. Two clearly visible peaks are due to the coupling of the fluorescence emission to either the TE or TM BSW mode, in agreement with the simulations shown in Fig. 1 [10,25]. The shape of the emission profile is related to the DyLight 650 emission spectrum via the dispersion of the TE and TM polarized BSW; for a given 1DPC design, it is therefore a characteristic signature of such a dye [27].

For each spot, the angularly dispersed fluorescence emissions in 50 adjacent CCD camera rows were acquired. Next, we subtracted the background fluorescence, followed by integrating the angular intensity distribution in each CCD row (Fig. 4) along the angle. Hence, the integral values are averaged over the 50 rows and assigned an intensity and standard deviation.

Biomedical Optics EXPRESS

5.3 Calibration assays

A calibration is needed to use the BSW platform for quantifying Ang2 levels in patients' plasma. For this purpose, duplicate standards of Ang2 were prepared in D-PBS by serial dilution of a stock solution of 0.1 mg/mL of Ang2 in D-PBS. Calibration data points were obtained for the following concentrations: 2.5, 5, 10, 20 and 50 ng/mL. The concentration was varied in such a range given that the Ang2 levels in cancer patients are generally higher than 1 ng/mL [6,46,47]. Pure D-PBS was used as a negative control. All calibration assays were performed with freshly bio-conjugated BSW biochips and in duplicate. In view of a clinical application of the platform, calibration with standards diluted in a matrix with complexity similar to that of human plasma will be needed.

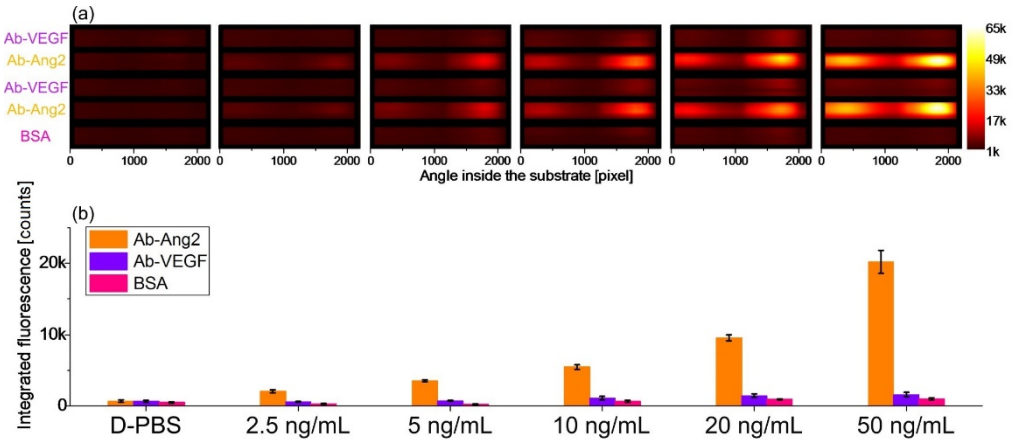

Fig. 5. Fluorescence intensities recorded for the standard Ang2 solutions at different concentrations in D-PBS. (a) Fluorescence intensities recorded by the CCD at the end of the assay. (b) Integrated and averaged intensities for each group of spots on the BSW biochip; the error bars represent the standard deviation associated with the integrated and averaged values.

Figure 5(a) shows the fluorescence intensities for each concentration recorded by the CCD. All measurements were carried out with the same CCD exposure time. When only D-PBS is injected during an assay carried out with exactly the same steps of the protocol (just without the target molecule), the platform detects a very low uniform signal from the whole surface. It also appears that any detection antibody, together with any NeutrAvidin 650 label, are non-specifically absorbed onto the sensor surface resulting in a non-specific fluorescence signal even after the background correction. However, the signal measured in the anti-Ang2 regions can be distinguished with a good contrast.

In Fig. 5(b), we plot the integrated and averaged fluorescence signal measured in analogues spots, i.e. the sensor area bio-conjugated with the same molecules. The bar plot shows increasing signal in response to the increasing Ang2 concentrations. Standard deviations of the mean values are calculated as the sum of the variances associated with the signal emitted from each region. Such standard deviations spread with increasing Ang2 concentration but relative values are constant. The overall response of the BSW platform is determined by the difference between the averaged intensities recorded in the Anti-Ang2 spots and in the reference spots. Figure 5(b) shows that the lowest Ang2 concentration of 2.5 ng/mL can be clearly detected.

The average overall responses of the two duplicate measurements carried out for each concentration, and their respective standard deviations calculated as the square root of the sum of the variances, can be plotted as a function of the Ang2 concentration, as shown in Fig. 6, and the resulting calibration curve can be used in assays with unknown Ang2 content.

Biomedical Optics EXPRESS

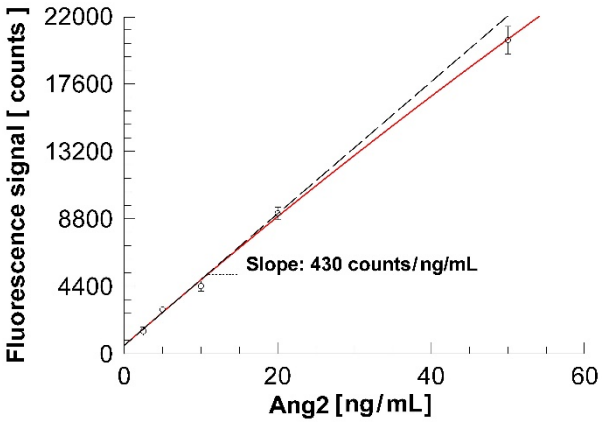

Fig. 6. Calibration curve of Ang2 in D-PBS. Each point represents the difference between the averaged intensities recorded in the Anti-Ang2 spots and in the reference spots averaged on two replicate measurements. The coefficient of variation (CV) of the data points is 18%, 6.5%, 7.3%, 4.5%, 4.4%, from the lowest to the highest concentration respectively.

5.4 Detection of Ang2 in human plasma samples

Applicability of the present sensor in clinics was investigated by quantifying Ang2 concentrations in human plasma samples from metastatic colorectal cancer patients. Each plasma sample was simultaneously validated by performing ELISA to quantify the Ang2 concentration in one aliquot. The ELISA tests on plasma samples collected from cancer patients before the therapy, showed an Ang2 median, minimum and maximum concentration of 4.5 ng/ml, 1.4 ng/ml, and 8.2 ng/ml, respectively.

Table 1. Ang2 concentrations in plasma samples from metastatic colorectal cancer patients as estimated by both the ELISA and the BSW platform. For the BSW system, each calculated value is the mean of two duplicate experiments.

	Detected Ang2 concentration [ng/mL]	
Plasma Sample	ELISA	BSW platform (σ)
S1	6.7	6.2 (0.4)
S2	5.7	5.8 (0.4)
S3	5.8	5.3 (0.2)

Among all the collected plasma, three samples (here reported as plasma S1, S2 and S3) were assayed with the BSW platform, dropping those with the largest and smallest Ang-2 concentration, as determined by the ELISA test. S1 and S2 were collected from the same patient before and during the therapy, respectively; while S3 was from a second patient after the therapy. The calibration curve shown in Fig. 6 was used to evaluate the Ang2 concentration from the averaged fluorescence intensities. For each plasma sample the assay was repeated twice, in different days and using fresh BSW biochips. The results are reported in Table 1 and compared to the values previously retrieved from ELISA assays carried out with the same plasma samples. The ELISA assays were carried out by the Quantikine Kit from R&D and according to the manufacturer's instructions; for such assays the plasma samples were 1:5 and 1:10 diluted.

Biomedical Optics EXPRESS

6. Discussion

The assays performed with the human plasma samples show that Ang2 can be detected by the BSW platform at clinically relevant concentrations in human plasma. A good agreement with the ELISA control assays is found, with a deviation of less than 10%, as shown in Table 1. Such a result demonstrates the good accuracy of the BSW platform to the standard laboratory tests such as ELISA.

According to both ELISA and BSW determination, the Ang2 concentration was around 5-6 ng/mL in all three human plasma samples.

Data reported in Fig. 6 can be fitted to a sub-linear calibration function, which can be then extrapolated to low concentration to evaluate the limit of detection (LoD) of the immunoassay implemented on the BSW platform in fluorescence mode. As a fitting function, we used a Langmuir isotherm model taking into account a background signal [26,48]:

$$F = A_1 + \frac{A_2 - A_1}{1 + A_3 / c} \quad (1)$$

where F is the measured fluorescence intensity, c is the Ang2 concentration, A_1 and A_2 are the background and maximum fluorescence intensities, respectively. Such a functional dependency accounts for the linear behavior at low concentration and for the sub-linear dependency at large concentration, which can be either due to the Langmuir model or also to the fact that the fluorescence signal produced by the 50 ng/mL solution almost saturated the CCD detector. The slope in the linear region in the limit of low concentration is S = (430 ± 77) counts / (ng/mL) and provides the sensitivity of the BSW platform in the fluorescence mode.

According to other methods commonly reported in literature [49,50], one can estimate the LoD = 2σ/S = (1.0 ± 0.2) ng/mL, where the standard deviation of the smallest concentration (σ = 220 counts) is used. The 2σ limit is consistent with the procedures used to evaluate the LoD of the ELISA method. The value of the estimated LoD is in our opinion reliable, since (1) the extrapolation interval is indeed small (from 2.5 to 1 ng/mL on a 50 ng/mL span), (2) the 2.5 ng/mL was clearly detected and (3) the platform's results coincide with the reference ELISA experiments. Together with the minimum concentration detected in the calibration assays (2.5 ng/mL), the estimated LoD is compatible with the concentration ranges of Ang2 in plasma from patients with colorectal cancer [6].

Table 2. Assay percent variations in plasma samples measurements and in the calibration procedure.

	Human plasma samples					*Mean*
	S1		S2		S3	
Relative variation of measured plasma samples [%]	6.68		7.23		3.18	5.70
	Calibration standards [ng/mL]					*Mean*
	2.5	5	10	20	50	
Relative variation of standards [%]	5.90	5.53	7.62	5.14	5.34	5.78

The BSW platform repeatability was assessed by evaluating the results obtained in the different assays, carried out with the same protocol for the same plasma sample. The relative variation for plasma sample measurements are reported in percent in Table 2. The table also presents the variability of the calibration procedure. As already mentioned, duplicate standards were prepared for each concentration (2.5, 5, 10, 20, 50 ng/mL) and were assayed

Biomedical Optics EXPRESS

with separate BSW biochips. Mean values of the relative variation are below 6% for both plasma measurements and standards. Moreover, all the individual values are below 10%, which is acceptable for an analytical method.

7. Conclusions

We demonstrated that the BSW biosensing platform described in the present work is suitable for the detection of relevant clinical levels of the angiogenic factor Ang2 in patient plasma samples. To the best of our knowledge this is the first BSW based biosensor assay for the determination of Ang2 in plasma samples at clinically relevant concentrations. The system takes advantage of BSW sustained by purposely designed 1DPC to excite and enhance a fluorescent immunoassay involving Ang2. The minimum Ang2 concentration in D-PBS that the platform detected is 2.5 ng/mL. The limit of detection in the fluorescence mode was evaluated to be (1.0 ± 0.2) ng/mL. Both values are compatible with clinically relevant Ang2 concentrations. The system is capable of assessing Ang2 concentration in plasma samples using small sample volumes (300 µL) with a short experimental time (30 minutes) and without sample pretreatment or dilution. The robustness was demonstrated by the good repeatability proven by low relative variation. The Ang2 plasma concentrations determined with the BSW system were validated by ELISA measurements and a good agreement between both the results was found, demonstrating the accuracy of our system. The limited number of plasma samples used in the present work does not yet permit to compare the developed BSW platform with a gold standard assay, since power regression analysis will have to be performed with a larger number of patient samples over a more extended Ang-2 concentration range. For this reason, at the present stage, we cannot correlate the concentration levels found with the platform to the clinical history of the patients. However, the outcome of the present work confirms that the BSW biosensing platform is a valuable tool for fast diagnosis of angiogenic factors and paves the way for the development of multiplexed BSW biosensors for the detection and monitoring of multiple clinical biomarkers.

Funding

This work was funded by the European Commission through the project BILOBA (Grant agreement 318035).

Disclosures

The authors declare that there are no conflicts of interest related to this article.